

E11851

Monte Carlo Simulation of Nanoparticle Encapsulation in Flames

Z. SUN, J.I. HUERTAS, and R.L. AXELBAUM
Washington University
St. Louis, Missouri

BACKGROUND

Gas-phase combustion (flame) synthesis has been an essential industrial process for producing large quantities of powder materials such as carbon black, titanium dioxide, and silicon dioxide. Flames typically produce simple oxides, with carbon black being the noted exception because the oxides of carbon are gaseous and are easily separated from the particulate matter that is formed during fuel pyrolysis. Furthermore, the powders produced in flames are usually agglomerated, nanometer-sized particles (nanoparticles). This composition and morphology is acceptable for many applications. However, the present interest in nanoparticles for advanced materials application has led to efforts to employ flames for the synthesis of *unagglomerated* nanoparticles (2 to 100 nm) of metals and non-oxide ceramics.

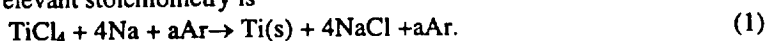
Sodium-halide chemistry has proven to be viable for producing metals and non-oxide ceramics in flames. Materials that have been produced to date include Si (Calcote and Felder, 1993), TiN, TiB₂, TiC, TiSi₂, SiC, B₄C (Glassman *et al.*, 1993) Al, W, Ti, TiB₂, AlN, and W-Ti and Al-AlN composites (DuFaux and Axelbaum, 1995, Axelbaum *et al.* 1996,1997). Many more materials are possible.

The main challenge that faces application of flame synthesis for advanced materials is overcoming formation of agglomerates in flames (Brezinsky, 1997). The high temperatures and high number densities in the flame environment favor the formation of agglomerates. Agglomerates must be avoided for many reasons. For example, when nanopowders are consolidated, agglomerates have a deleterious effect on compaction density, leading to voids in the final part. Efforts to avoid agglomeration in flames without substantially reducing particle number density and, consequently, production rate, have had limited success.

Another critical challenge that faces all synthesis routes for nanopowders is ensuring that the powders are high purity and that the process is scaleable. Though the containerless, high temperature environment of a flame is excellent for producing high-purity simple compounds, ultrafine metals and non-oxide ceramic powders are inherently reactive in the presence of oxygen and/or moisture. Thus, the handling of these powders after synthesis poses a challenging problem. Impurities acquired during handling of nanoparticles have plagued the advancement of nanostructured materials technology.

One promising approach that has been proposed to address these problems is nano-encapsulation (DuFaux and Axelbaum, 1995). In this approach, the *core* particles are encapsulated in a removable material while they are within the flame but before excessive agglomeration has occurred. Condensation can be very rapid so that core particles are trapped within the condensed material and subsequently agglomeration is limited. Figure 1 shows transmission electron microscope (TEM) micrographs of powders produced with a nano-encapsulation process in sodium-halide flames.: titanium (Fig. 1a,b) and aluminum nitride (Fig. 1c). These results demonstrate nano-encapsulation and, as can be seen from Figs. 1a and b, the size of the core particles can be varied by controlling process conditions.

For synthesis of titanium metal the relevant stoichiometry is



For these flames the NaCl by-product, the lighter material in the micrographs, acted as the encapsulation material and the argon is added to control encapsulation, as will be discussed.

Another significant advantage of nano-encapsulation is in handling during post-production processing. Results have shown that when the powders are exposed to atmosphere the core particles are protected from oxidation and/or hydrolysis. Thus, handling of the powders does not require extreme care. If, for example, at the time of consolidation the encapsulation material is removed by vacuum annealing, the resulting powders remain unagglomerated and free of impurities.

MODELING

Modeling aerosol dynamics such as that occurring in sodium halide flames, where core particles are encapsulated following rapid condensation of a second component, requires that a multicomponent aerosol model be developed. The objective is to predict both the final particle size and the size of the core particles under conditions of simultaneous coagulation and condensation. The sectional method is an established technique for modeling coagulation alone and some efforts have been made to extend this technique to allow for condensation. However, the sectional method when applied to condensation suffers from numerical diffusion or dispersion because condensed mass is distributed over the entire section and there is a flux of mass across the grid boundaries. The need exists for an alternative, more robust approach to modeling aerosol processes with simultaneous coagulation and condensation. Furthermore, the sectional

method yields integrated quantities describing the composition of particles in a given section. For this work we require not only composition but also the size and number of core particles in the particle, i.e., we require the size distribution of core particles within a section. To this end, a Monte Carlo scheme has been developed which affords a statistical treatment of coagulation coupled with a deterministic treatment of condensation and evaporation. Numerical diffusion and dispersion are avoided because the method solves for both mass and number, and a moving grid avoids flux of condensable mass across the grid boundary. The Monte Carlo approach is ideally suited to a moving grid approach and the addition of a moving grid does not entail significant complexity.

The details of the method are given in Huertas *et al.* (1998) and are only summarized below. For a given size distribution the probability of collision is determined for a discrete size interval (grid) and the Monte Carlo method is used to statistically solve for the evolution due to collisions. Condensation and evaporation, on the other hand are solved classically by integrating appropriate rate equations. This input is coupled to the Monte Carlo scheme by calculating the time between collision events.

Only binary collisions are considered and the collision frequency between particles of size i and j is given by $Z_{ij} = \beta_{ij}N_iN_j$, where β_{ij} is the collision frequency factor and N is the number density. The probability that a collision of type i - j occurs is $q_{ij} = \beta_{ij}N_iN_j / \sum \beta_{ij}N_iN_j$. In time step δt there are a total of $p = \sum \beta_{ij}N_iN_j \delta t$ collisions. To update a size distribution over a time step δt , p collisions are randomly chosen based on their probabilities and the distribution is updated accordingly. Since the aerosol under consideration has two components and we required not only the composition of the particles but also the distribution of core particles within the particle, we retain $N(d_i, Y_i)$, $m_1(d_i, Y_i)$ and $m_2 N(d_i, Y_i)$, where m_k is the mass distribution function of component k . For example, if component 1 is NaCl and 2 is AlN we seek the size distribution of AlN particles encapsulated within salt particles.

For the high rates of condensation required for effective encapsulation, it is necessary to avoid errors associated with numerical diffusion and dispersion. With the Monte Carlo method the particle size associated with grid i is not prescribed, but rather a mass mean diameter is determined based on the mass and number of particles within grid i . Condensation will cause the mass mean diameter of grid i to grow to a defined larger value and, from this perspective, numerical diffusion is avoided. Nonetheless, if the grids are fixed, the growth of the mass mean diameter beyond the boundaries of a grid would lead to numerical dispersion which would result in peaks and valleys in the number density distribution. This difficulty can be avoided by employing a moving grid approach wherein the grid boundaries grow in accordance with growth of a particle of similar size. Thus, condensation does not result in mass transfer across the grid boundary and the common difficulty of modeling condensation in coagulating aerosols is avoided.

RESULTS

Coagulation results were verified by comparing to the Smulochowski solution as well as published numerical and experimental results. Factors that can affect numerical accuracy of this model are the number and distribution of sections, the number of particles that are used to represent the aerosol (i.e., the sample volume considered), and the time step for upgrading the size distribution. With greater than 18 sections per division the results are not dependent on number of sections. The number of particles decreases due to coagulation and to maintain satisfactory statistics the code allows the number of particles to decrease by one order of magnitude and then rescales the system to the original number of particles (i.e., a larger sample volume is used.) Typically 10^5 to 10^6 particles is sufficient to maintain accuracy.

Figure 2 illustrates how numerical dispersion can be eliminated by employing a moving grid. The dashed line is the original size distribution prior to condensation and the solid line is the calculated distribution 20 ms later, obtained with fixed (Fig. 2a) and moving (Fig. 2b) grids. The concentration of condensable mass used in this calculation is typical for sodium-halide flame synthesis and a heat loss of 2 W/cm^3 was assumed. As seen in Fig 2a, when the grid is fixed, numerical dispersion yields an oscillatory distribution about the true distribution obtained with a moving grid (Fig. 2b.)

For simplicity, the particle encapsulation process relevant to sodium-halide combustion will be modeled assuming a homogeneous closed system. The actual flame is a complex process involving diffusive and convective transport and reaction. Nonetheless, the salient features of encapsulation can be understood without detailed modeling of the flame and the usefulness of the Monte Carlo method can be demonstrated in this way.

From the chemistry of Eq. 1, it is clear that one component, in this case Ti, has a low vapor pressure (10^{-7} mm Hg at 1473 K) and will rapidly condense out at the flame. The other component, the encapsulation material, NaCl, has a high vapor pressure (84 mm Hg at 1473 K) and can be in either the vapor or condensed phase, depending on temperature and α , the stoichiometric coefficient for the inert in Eq. 1. Flame temperature can be controlled by heat loss and reactant dilution and is typically around 1373 K, which is sufficiently high that the NaCl is initially in the vapor phase. As the particles are convected away from the flame, they rapidly cool due to radiation and entrainment. This

decrease in temperature drives the salt out of the vapor phase. A heat loss of $1\text{--}2\text{ W/cm}^3$ is possible in these particle laden flames and for the purposes of illustration we will assume 2 W/cm^3 .

Figure 3 shows the particle evolution of the aerosol at times just prior to salt condensation ($t = 0\text{ ms}$) and 50 and 400 ms later (Figs. 3a - c, respectively.) The particle size distribution shown in Fig. 3a, which is for Ti particles, was found to be independent of initial size distribution. The total mass of Ti in the aerosol is prescribed by Eq. 1 with $a = 50$ and $p = 1\text{ atm}$. Following the onset of condensation, the aerosol quickly evolves to a bimodal size distribution, the smaller particles being Ti and the larger particles being largely NaCl. The size distribution of the NaCl particles is effectively frozen in time while that of Ti rapidly decays as the Ti particles collide with the large salt particles.

In Fig. 4 we see the early stages of the evolution that lead to the bimodal size distribution. Prior to condensation the critical size d^* is effectively infinite but with high heat loss it rapidly decreases (Fig. 5), reaching the tail of the Ti size distribution. As d^* reduces further condensation begins and since this is a closed system the amount of NaCl in the vapor phase decreases. Initially the heat loss is able to continue reducing d^* and smaller particles are coated, but as the vapor phase NaCl is depleted, d^* reaches a minimum and then increases.

The encapsulation process can be summarized as follows. The core or primary particles (Ti in this example) form in the flame and evolve normally as they would without a second phase. At the onset of condensation a small fraction of the particles in the tail of the distribution act as heterogeneous nucleation sites for the condensable vapor (NaCl) and are coated. These coated particles rapidly consume the NaCl and due to the Kelvin effect they are the only particles that receive additional condensate. These "salt" particles grow very large because of the large amount of NaCl in the products (see Eq. 1) and they act to scavenge the remaining Ti particles.

Three possible structures can be formed within the scavenging particles. First, the core particles can remain separate, as would occur if times prior to solidification of the melt are short (the melting point of NaCl is 1073 K), and this we term the frozen solution. In addition, if the core particles collide within liquid NaCl they can either form small aggregates or fully coalesce within the NaCl matrix. Referring back to Fig. 1, we see indications of all three. The powder produced with cool reactor walls (Fig. 1a) shows ca. 10 nm particles embedded in NaCl, indicating a frozen case. At flame conditions that lead to higher temperatures and with heated walls the particles are larger (Fig. 1b) presumably due to collision in liquid phase and subsequent coalescence. The AlN particles in Fig. 1c appear to be small aggregates.

An important aspect of the Monte Carlo model is that it retains a record of collisions. Thus, not only can the composition be obtained as a function of size, but the size of the core particles within a scavenging particle can be obtained. Thus in the limit of the frozen solution we can obtain the size distribution of core particles and this is shown in Fig. 6. The frozen solution shows that in this limit the encapsulation process clips the tail of the size distribution, leading to a narrow size distribution.

ACKNOWLEDGMENTS

This work was supported under NASA Grant NAG3-1910.

REFERENCES

- Axelbaum, R.L., Huertas, J.I., Lottes, C.R., Hariprasad, S. and Sastry, S.M.L., (1996) *Materials and Manufacturing Processes*, 11(6): 1043-1053.
- Axelbaum, R.L., Lottes, C.R., Huertas, J.I and Rosen L.J. (1997) *Twenty-Fifth Symposium (International) on Combustion*.
- Brezinsky, K. (1997) *Twenty-Fifth Symposium (International) on Combustion*.
- Calcote, H.F. and Felder, W. (1993) *Twenty-Fourth Symposium (International) on Combustion*, The Combustion Institute, pp.1869-1876.
- DuFaux, D.P. and Axelbaum, R.L. (1995) *Combustion and Flame*. 100:350-358.
- Gelbard, F. (1990) *Aerosol Science and Technology*, 12: 399-412.
- Glassman, I., Davis, K.A. and Brezinsky, K. (1993) *Twenty-Fourth Symposium (International) on Combustion*, The Combustion Institute, pp. 1-14.
- Huertas, J.I., Sun, Z. and Axelbaum, R.L., (1998) In preparation.
- Seinfeld, J.H. (1986) *Atmospheric Chemistry and Physics of Air Pollution*, John Wiley, NY.
- Warren, D.R. and Seinfeld, J.H. (1985) *Aerosol Science and Technology*, 4: 31-43.



Figure 1. NaCl encapsulated particles produced in sodium/halide flames: (a) titanium, (b) titanium produced at higher temperature and (c) aluminum nitride. The dark particles are the core particles and the lighter material is the NaCl encapsulation.

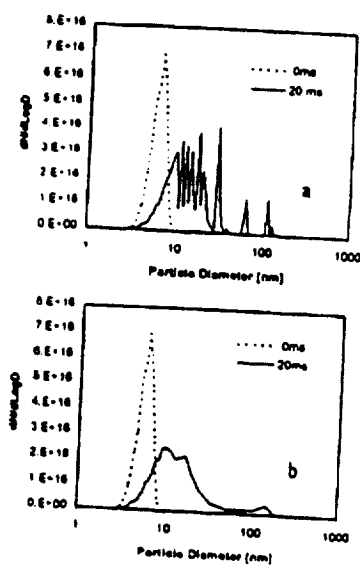


Figure 2. Monte Carlo solution of simultaneous coagulation and condensation with (a) fixed grid and (b) moving grid. The fixed grid leads to numerical dispersion.

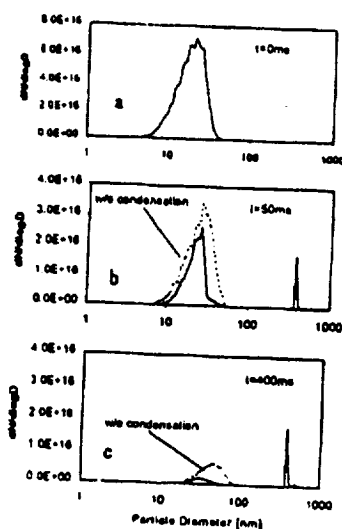


Figure 3. Evolution of aerosol undergoing rapid condensation of a second phase. The dashed line shows the evolution of the distribution without condensation.

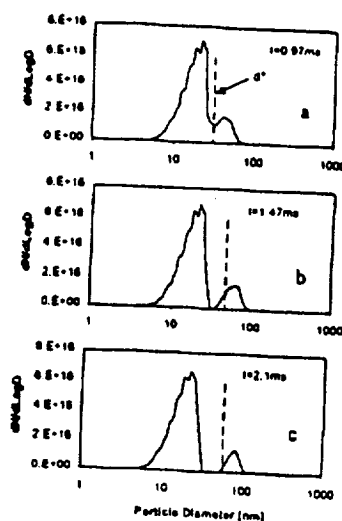


Figure 4. The early stages of condensation for the aerosol of Fig. 3 showing the development of a bimodal size distribution.

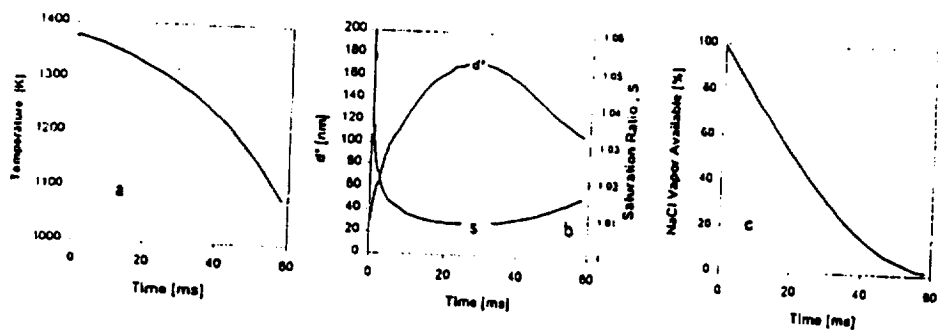


Figure 5. Evolution of (a) temperature, (b) d' and S , and (c) NaCl remaining in the vapor phase.

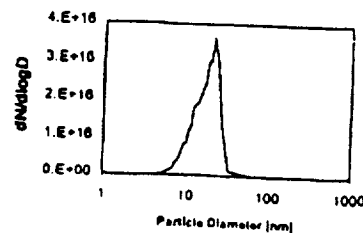


Figure 6. Distribution of core particles under a frozen solution, i.e. no collisions of core particles within the scavenging particles.